Impact of substrate pits on laser-induced damage performance of 1064-nm high-reflective coatings

Yingjie Chai,[1,2] Meiping Zhu,[1,*] Zhengyuan Bai,[1,2] Kui Yi,[1] Hu Wang,[1,2] Yun Cui,[1] and Jianda Shao[1]

[1]*Key Laboratory of Materials for High Power Laser, Shanghai Institute of Optics and Fine Mechanics, No. 390 Qinghe Road, Jiading District, Shanghai 201800, China*

[2]*Graduate School of Chinese Academy of Sciences, Beijing 100039, China*

**Corresponding author: bree@siom.ac.cn*

Received December 10, 2014; revised February 12, 2015; accepted February 13, 2015; posted February 18, 2015 (Doc. ID 230503); published March 23, 2015

The laser damage resistance of coatings in high-power laser systems depends significantly on the surface quality of the substrate. In our experiment, pits were precisely fabricated on the surface of fused silica substrate using a femtosecond laser processing bench. The HfO_2/SiO_2 high-reflective coatings at 1064 nm were deposited by conventional e-beam evaporation onto fused silica substrates with and without pits, respectively. The internal crack that was induced by the substrate geometrical structure was first observed in our experiment. The laser-induced damage threshold test showed negative effects of the substrate pits on the laser resistance of high-reflective coatings. Simulations by the finite element method were carried out, and results demonstrated that the modulation of a high reflector multilayer geometry could lead to electrical-field amplification and reduce laser damage resistance. Combined with its poor mechanical properties, the pits on substrate could contribute to the occurrence of damages. © 2015 Optical Society of America

OCIS codes: (140.3330) Laser damage; (220.4000) Microstructure fabrication; (310.6870) Thin films, other properties.
http://dx.doi.org/10.1364/OL.40.001330

HfO_2/SiO_2 multilayer dielectric thin films with e-beam deposition are widely used in 1064-nm high-power laser systems because of their high laser damage resistance. However, HfO_2/SiO_2 coatings are fluence-limited by rare failures induced by nanosecond laser irradiation with a wavelength of 1064 nm, which limit the quality of the current low-defect density mirrors. Defects on the substrate are believed as one of the most important factors in limiting coating function and lifetime, such as scratches [1], impurities [2–6], and pits [7] on the substrate. Defects on the substrate surface were mainly created during the final shaping of the component through abrasive cutting, grinding, and final polishing [8]. Several studies focused on the correlation between the type of substrate defects and laser-induced damage threshold (LIDT) [9–14]. The disruptions in the film structure resulting from high or low points on the substrate surface (particles [8,9]/engineered defects [10–13] or scratches [1]/pits [7]) lead to enhancements in the electric-field intensity and a corresponding negative impact on laser damage thresholds. The same attention should be concerned on the scratches and pits on substrate as well as nodule, in both damage morphologies and mechanism. The correlation between LIDT and the physical properties of substrate scratches was delineated by experiment, and the laser-induced damage occurs on the region of the coatings where substrate scratches reside [1]. Generally, the scratches were created by dragging the sample surface across a pad that contained imbedded silica spheres in different size with the disadvantage of generating cracks near the structural defect [14]. The scratch width of 15–60 μm are investigated, which should not be existed in actual coating process. After the laser irradiation, the pit and delamination in the damage sites could be investigated to find the possible reasons leading to damage [15]. Defect features in the multilayer coatings originating from substrate surface play important roles in limiting the laser damage resistance.

This report focuses on the damage of HfO_2/SiO_2 multilayer coatings induced by the pits on substrate. The role of laser-induced damage in optical materials can be both negative (a factor that limits the resistance of laser-induced damage performance in high-power laser system) and positive (providing a tool for material fabrication and modification). In our experiment, an 800-nm-femtosecond laser was used for fabricating micro-pits on the substrate, and a 1064-nm-nanosecond laser was used for damage testing. The pits were precisely fabricated by femtosecond laser to prevent the emergence of subsurface cracks, which might be induced during cold machining process. The high-reflective (HR) coatings were then coated on the substrates with and without pits, and the LIDT was tested. The damage morphologies by a nanosecond laser with a wavelength of 1064 nm were shown to indicate the damage process and the cause of damage. A theoretical study was designed to investigate the influence of $|E|^2$ distributions on the damage behavior of the coatings on the pits. Our results demonstrated exactly that the impact of pits defects affect the damage behavior of HR coatings.

All experiments were conducted on fused silica with dimension of 50 mm in diameter and 5 mm in thickness, which exhibits less than 0.8 nm of RMS surface roughness after an ultrasonic bath. The femtosecond fabrication technique used has been introduced in [7,16]. The SEM micrographs on the region fabricated by femtosecond processing are shown in Fig. 1. The mesh spacing is 300 μm for the alignment of laser irradiation during LIDT. The pit spacing is 18 μm, with lateral size of ~7 μm and vertical size of 3 μm. Further observation with cross-sections of the pits by a focus ion beam showed no crack below the pits.

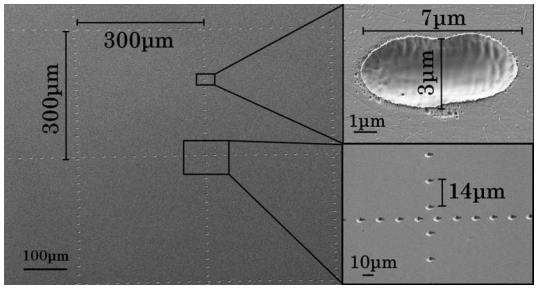

Fig. 1. SEM micrographs of the rectangular mesh fabricated by 800-nm-femtosecond laser.

HR coatings with a multilayer structure Sub/4L(HL)^{11} H4L/air were deposited on the substrates with and without the femtosecond laser fabricated pits. HfO_2 and SiO_2 are chosen as high- (H) and low- (L) refractive index materials, and H and L have a quarter-wave optical thickness at the reference wavelength of 1064 nm.

LIDT testing was performed in the "1-on-1" regime according to the ISO standard 21254-1, using a pulsed Nd:YAG laser operating with a pulse duration of 12 ns at 1064 nm with normal incident angle. The experimental setup was detailed in Refs. [17,18]. The laser radiation at the sample plane had a near-Gaussian spatial profile with an effective diameter of about 397 μm. The damage morphologies were characterized by a focused ion beam-scanning electron microscope (FIB-SEM, Carl Zeiss AURIGA Cross Beam).

The typical morphology of the coatings on the pits was observed by SEM and a cross-section of the pits by FIB showed in Fig. 2. For the 1064 nm HR coatings structural defect (length: ~7 μm; width: ~3 μm; depth: 800 nm), cracks were observed in the relatively deeper layer of the film, which resulted in a discontinuous geometric structure. The LIDT testing of the two kinds of samples were evaluated and compared, as shown in Fig. 3.

The pits on the substrate significantly decreased the LIDT of the HR coatings. The damage in the HR coatings of the samples without pits was extremely rare. As shown in Fig. 4 a single shot of 1064-nm laser with high fluence of 151 J/cm^2 caused a small nodule ejection morphology with a large area of plasma scald. However, damage of the HR coatings was observed after laser irradiation with fluence of 40 J/cm^2, which also showed the morphology of plasma scald whose source is definitely located in the position of pit defects. As shown in Fig. 5, the groove bottom of the pit site on coating surface was seriously

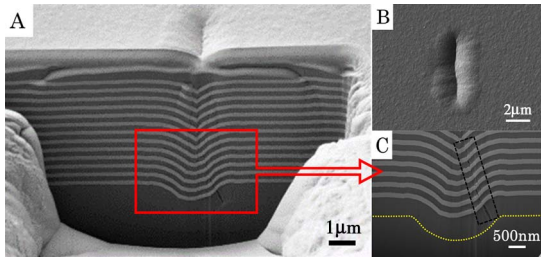

Fig. 2. Typical morphology of HR coatings with pits by SEM. (A) and (C) Cross-section of the pits section. The yellow dashed line indicates the interface of the film and the substrate. (B) Surface morphology of pits section after e-beam deposition.

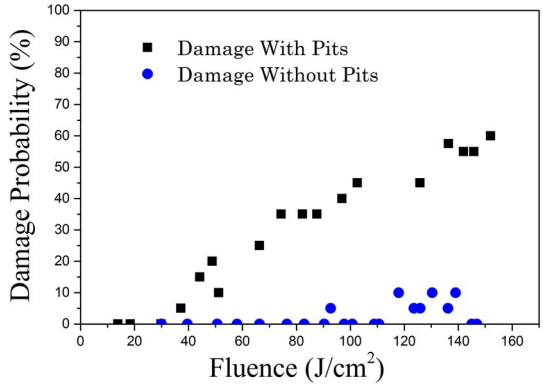

Fig. 3. 1-on-1 LIDT testing result of HR coatings deposited on substrate with and without pits.

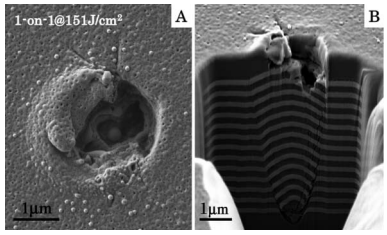

Fig. 4. (A) SEM microgram of the damage site of HR coatings deposited on the fused silica without pits at fluence of 151 J/cm^2; (B) cross-section of the damage site.

damaged with the irradiation of low laser fluence, and the meltdown mostly occurred possibly because of the rapid elevation of temperature during the irradiation induced by E-field intensification. After high fluence laser irradiation, the negative impact of cracks in deep coating layers are obvious, which is observed by FIB (Fig. 5).

To elucidate, if the substrate pits can lead to E-field intensification within the HR coatings, a cross-sectional image of HfO_2/SiO_2 was used to estimate the E-field distribution by finite element method (FEM). The distribution images of E-field intensity $|E|^2$ were plotted in

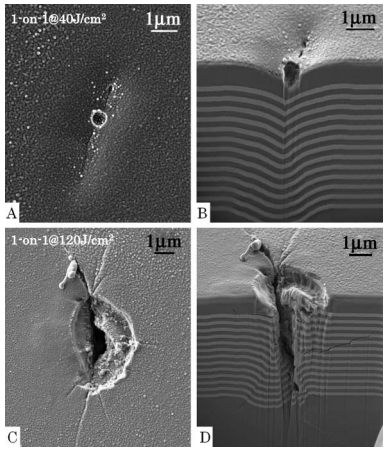

Fig. 5. (A) SEM microgram of the damage site of HR coatings deposited on the fused silica with pits at low fluence of 40 J/cm^2; (B) cross-section of the damage site (A). (C) SEM microgram of the damage site of HR coatings deposited on the fused silica with pits at high fluence of 120 J/cm^2; (D) cross-section of the damage site (C).

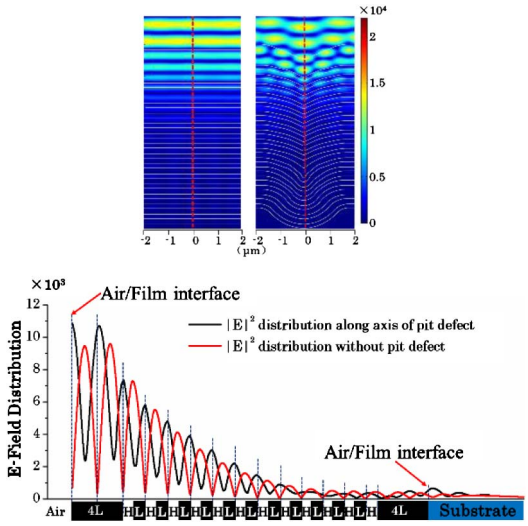

Fig. 6. FEM simulated $|E|^2$ distribution for pits under consideration: $|E|^2$ distribution of HR coatings without pit and HR coatings with pit. The color scales are the same; $|E|^2$ distribution along the coating far away from the defect and along the axis of the coating.

Fig. 6, and the color scale indicates the E-field strength. The HR coatings changes its morphology accordingly while trying to recover its flatness. The profile of refractive index was got by image process with SEM-FIB figure. The refractive index values (1.45 for SiO_2 and 1.94 for HfO_2) are estimated by the commercial thin-film design software Essential Macleod. As shown in Figs. 6 and 8(D), the highest E-field intensifications are located at the groove bottom of the pit site in air/film interface. The pit defects resulted in an $|E|^2$ enhancement that was ~17 times higher than the incident field strength near the interface of air and film. The distorted coatings caused by the existence of the pit in the substrate easily caused damage when irradiated by a laser. The temperature distribution in the whole laser irradiated region [19] shown in Fig. 7 can be described as (1)

$$\begin{aligned} C_n\left(\frac{\partial T(r,z,t)}{\partial t}\right) - K_n\nabla^2 T(r,z,t) &= Q(r,z,t);\\ \frac{\partial T(r,z=0,t)}{\partial t} &= \gamma T(r,z=0,t);\\ T(r,z=\infty,t) &= T(r=\infty,z,t) = 0;\\ T(r,z,t=0) &= 0, \end{aligned} \tag{1}$$

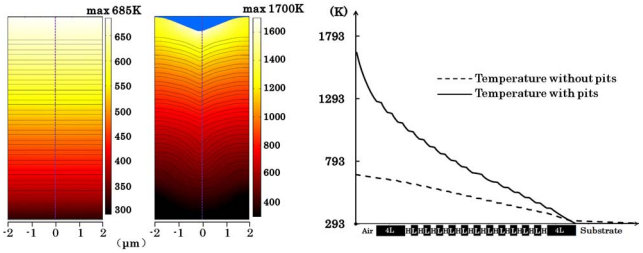

Fig. 7. Thermal simulation of temperature for the pits defects; temperature distribution of HR coatings without pit and HR coatings with pit; temperature distribution along the coatings with and without pits.

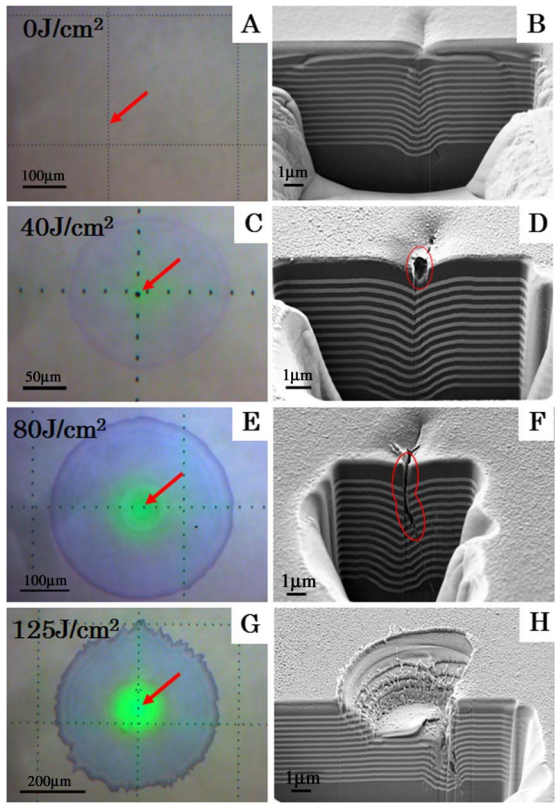

Fig. 8. Optical microscope images and cross-section of damage sites (incidence angle 0°, 1-on-1 at 1064 nm) at laser fluence: (A) and (B) no laser irradiation; (C) and (D) 40 J/cm^2, the groove bottom is marked by red circle; (E) and (F) 80 J/cm^2, the damage cracks is marked by red circle; (G) and (H) 125 J/cm^2.

where C_n is the specific heat, K_n is the heat conductivity, γ is heat exchange coefficient, and $Q(r,z,t)$ is the heat generated by absorption both from layers and interfaces. Without considering the absorptive defects in multilayer coatings, the intrinsic damage threshold is limited by the electric-field-induced thermal damage of the coating materials. The extinction coefficient of the adhesion layer is much higher than the intrinsic parameter [20–23]. The extinction coefficient used in the simulation were 7×10^{-5} for HfO_2, 1×10^{-5} for SiO_2, 5×10^{-2} for the interface of layer/layer, and 8×10^{-2} for the interface of air/layer. The structure with pits reached a much higher temperature gradient when irradiated by the same laser fluence. In addition, cracks were observed in the coatings, and stress damage occurred more easily when

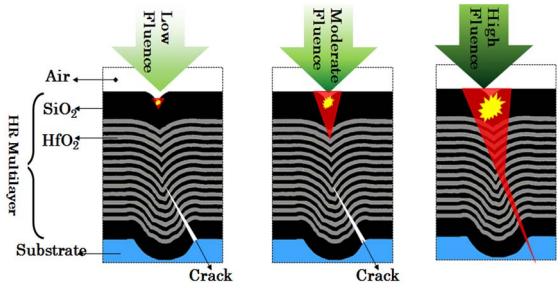

Fig. 9. Schematic diagram of phenomenological model to describe the formation of the laser induced damage.

the temperature gradient was larger. This is the reason why the bottom region of the coatings is easily damaged with low fluence.

The damage caused by substrate pits on HR coatings upon laser exposure could be explained by different factors. According to the thermal transfer theory, a phenomenological model is proposed to describe the formation of the damage. As shown in Figs. 8 and 9, irradiation by low fluence laser pulse heated the air/SiO_2 interface of pit defect into a high temperature. As a result, an extremely unstable nanoabsorbing center is revealed by pit surface meltdown. When the irradiation fluence increase, the range of damage increases both laterally and vertically with expanding plasma scald. When the damage penetrates into the cracked region, the damage extended into the substrate very quickly, which eventually lead to destruction of the multilayer structure.

In this experiment, pits on the substrate were fabricated using a femtosecond laser, which dictated the modulation of a high-reflector multilayer geometry, and can lead to electrical-field amplification and reduced laser damage resistance. The cause of damage on the HR coatings with pits is the combination of electric field intensification, temperature rising, and stress release of crack in the thin film. Moreover, pits defects of ~3 μm in width and ~800 nm in depth were fabricated and tested, which was particularly easy to generate damage on HR coatings over the range of fluence tested in this study. The combination of E-field and intensification and poor mechanic structure (internal cracks in HR coatings) eventually induced the catastrophic damage. Through this work, we have ascertained that the micro-scale pits on the substrate are one of the sources of damage on thin film. It could not be ignored, and much more attention should be deserved, which can help researchers improve the LIDT of optical film coatings.

The authors would like to express their gratitude to Prof Zhengxiu Fan for the helpful discussion and to acknowledge the support of Xiaofeng Liu, Lin Zou, and Wenwen Liu in preparing this manuscript. The authors would like to acknowledge Zhilong Cai who helped prepare the femtosecond fabricated samples and Dawei Li in the LIDT test. This work is supported by the National Natural Science Foundation of China under Grant No. F050602 and International Science & Technology Cooperation Programs of China (2012DFG51590).

References

1. S. R. Qiu, J. E. Wolfe, A. Monterrosa, W. A. Steele, N. E. Teslich, M. D. Feit, T. V. Pistor, and C. J. Stolz, Proc. SPIE **7842**, 78421X (2010).
2. S. Wu, J. Shao, K. Yi, Y. Zhao, and Z. Fan, Rare Metal Mat. Eng. **5**, 757 (2006).
3. Z. Yu, H. He, W. Sun, H. Qi, M. Yang, Q. Xiao, and M. Zhu, Opt. Lett. **38**, 4308 (2013).
4. L. Wu, C. J. Stolz, S. C. Weakley, J. D. Hughes, and Q. Zhao, Appl. Opt. **40**, 1897 (2001).
5. L. Gallais, J. Capoulade, J. Y. Natoli, and M. Commandré, J. Appl. Phys. **104**, 053120 (2008).
6. J. Y. Natoli, L. Gallais, B. Bertussi, A. During, M. Commandré, J. L. Rullier, F. Bonneau, and P. Combis, Opt. Express **11**, 824 (2003).
7. Y. Chai, M. Zhu, K. Yi, H. Qi, H. Wang, W. Sun, Z. Yu, Z. Bai, Y. Zhao, and J. Shao, Proc. SPIE **9237**, 92370 (2014).
8. J. Yang, K. Yi, C. Wei, G. Hu, H. Cui, and J. Shao, High Power Laser Particle Beams **26**, 072011 (2014) (in Chinese).
9. C. J. Stolz, M. D. Feit, and T. V. Pistor, Appl. Opt. **45**, 1594 (2006).
10. X. Cheng, A. Tuniyazi, J. Zhang, T. Ding, H. Jiao, B. Ma, Z. Wei, H. Li, and Z. Wang, Appl. Opt. **53**, A62 (2014).
11. L. Gallais, X. Cheng, and Z. Wang, Opt. Lett. **39**, 1545 (2014).
12. X. Cheng, Z. Shen, H. Jiao, J. Zhang, B. Ma, T. Ding, J. Lu, X. Wang, and Z. Wang, Appl. Opt. **50**, C357 (2011).
13. C. J. Stolz, J. E. Wolfe, J. J. Adams, M. G. Menor, N. E. Teslich, P. B. Mirkarimi, J. A. Folta, R. Soufli, C. S. Menoni, and D. Patel, Appl. Opt. **53**, A291 (2014).
14. P. E. Miller, J. D. Bude, T. I. Suratwala, N. Shen, T. A. Laurence, W. A. Steele, J. Menapace, M. D. Feit, and L. L. Wong, Opt. Lett. **35**, 2702 (2010).
15. X. Liu, Y. Zhao, Y. Gao, D. Li, G. Hu, M. Zhu, Z. Fan, and J. Shao, Appl. Opt. **52**, 2194 (2013).
16. Y. Liao, Y. Ju, L. Zhang, F. He, Q. Zhang, Y. Shen, D. Chen, Y. Cheng, Z. Xu, K. Sugioka, and K. Midorikawa, Opt. Lett. **35**, 3225 (2010).
17. Z. Yu, H. He, X. Li, H. Qi, and W. Liu, Chin. Opt. Lett. **11**, 073101 (2013).
18. J. Liu, W. Zhang, H. Cui, J. Sun, H. Li, K. Yi, and M. Zhu, Chin. Opt. Lett. **12**, 083101 (2014).
19. M. Mansuripur, G. A. Neville Connell, and J. W. Goodman, Appl. Opt. **21**, 1106 (1982).
20. H. Bennett and D. K. Burge, J. Opt. Soc. Am. **70**, 268 (1980).
21. X. Tang, Z. Fan, and Z. Wang, Opt. Eng. **33**, 3406 (1994).
22. J. Lu, X. Cheng, Z. Wang, and H. Liu, Opt. Eng. **51**, 121814 (2012).
23. M. Zhu, K. Yi, D. Li, X. Liu, H. Qi, and J. Shao, Opt. Commun. **319**, 75 (2014).